Murine norovirus-1 cell entry is mediated through a non-clathrin, non-caveolae, dynamin and cholesterol dependent pathway

Andreas Gerondopoulos [1, 3], Terry Jackson [2], Paul Monaghan [2,4] Nicole Doyle [1] and Lisa O. Roberts [1*]

[1] Faculty of Health and Medical Sciences, University of Surrey, Guildford, Surrey GU2 7XH, UK

[2] Institute for Animal Health, Ash Road, Pirbright, Woking, Surrey GU24 0NF, UK

[3] Present address: University of Liverpool, Cancer Research Centre, 200 London Road, Liverpool L3 9TA, UK

[4] Present address: Australian Animal Health Laboratory, 5, Portarlington Road, Geelong VIC 3220, Australia

*Author for correspondence. Tel: 44 1483 686499; Fax: 44 1483 300374;

e-mail: l.roberts@surrey.ac.uk

Running title: Murine norovirus-1 cell entry

Keywords: norovirus, endocytosis, clathrin, dynamin, cholesterol

No. words in summary: 225

No. words in text: 5451

No. figures: 6

Summary

For many viruses, endocytosis and exposure to the low pH within acidic endosomes is essential for infection. It has previously been reported that FCV uses clathrin-mediated endocytosis for entry into mammalian cells. Here we report that infection of RAW264.7 macrophages, by the closely related murine norovirus-1, does not require the clathrin pathway, as infection was not inhibited by expression of dominant-negative Eps15 or by knock down of the AP-2 complex. Further, infection was not inhibited by reagents that raise endosomal pH. RAW264.7 macrophages were shown not to express caveolin, and flotillin depletion did not inhibit infection, suggesting that caveolae and the flotillin pathway are not required for cell-entry. However, MNV-1 infection was inhibited by methyl-β-cyclodextrin and the dynamin inhibitor, dynasore. Addition of these drugs to the cells after a period of virus internalisation did not inhibit infection, suggesting the involvement of cholesterol sensitive lipid-rafts and dynamin in the entry mechanism. Macropinocytosis was shown to be active in RAW264.7 macrophages (as indicated by uptake of dextran) and could be blocked by EIPA, which is reported to inhibit this pathway. However, infection was enhanced in the presence of EIPA. Similarly, actin disruption, which also inhibits macropinocytosis, resulted in enhanced infection. These results suggest that macropinocytosis could contribute to virus degradation or that inhibition of macropinocytosis could lead to the up-regulation of other endocytic pathways of virus uptake.

Introduction

The *Caliciviridae* are divided into four genera; *Vesivirus, Lagovirus, Sapovirus* and *Norovirus*. The human noroviruses are the most common cause of acute viral gastroenteritis, especially in industrialised countries (Lopman *et al.*, 2003); there is currently no treatment or vaccine for these viruses. In addition, there is still no routine tissue culture system for the propagation of human noroviruses, but the recent discovery of murine norovirus-1 (MNV-1) has provided an efficient model system for the study of norovirus replication, as this virus replicates efficiently in murine macrophages and dendritic cells (DCs) (Karst *et al.*, 2003; Wobus *et al.*, 2004). MNV-1 is highly prevalent in laboratory mice and has been shown to be lethal to mice with impaired innate immunity (Hsu *et al.*, 2006; Karst *et al.*, 2003; Muller *et al.*, 2007).

Noroviruses are non-enveloped and contain a single- stranded RNA genome of about 7.3 kb, which is linked to the viral VPg protein at the 5' end and is polyadenylated at the 3' end (Karst *et al.*, 2003; Wobus *et al.*, 2004). The genome is organised into 4 open-reading frames (ORF1-4). ORF-1 encodes the non-structural proteins whereas ORF-2 and ORF-3 encode structural proteins (Sosnovtsev *et al.*, 2006). ORF-4 was recently identified within the MNV-1 genome and encodes a single protein of unknown function (Thackray *et al.*, 2007).

For many viruses, infection requires virus uptake by endocytosis. A number of different endocytic pathways have been identified in mammalian cells. Broadly, these are divided into clathrin-mediated endocytosis and clathrin-independent endocytosis (CIDE) pathways which include caveolin-dependent endocytosis (or caveolae-mediated endocytosis) and a number of caveolin-independent pathways such as macropinocytosis,

and the flotillin-dependent and CLIC/GEEC (clathrin-independent cargos/GPI-AP-enriched early endosomal compartment) pathways (Glebov *et al.*, 2006; Marsh & Helenius, 2006; Miaczynska & Stenmark, 2008). CIDE pathways show different requirements for cellular proteins such as dynamin, flotillin and small GTPases (Glebov *et al.*, 2006; Marsh & Helenius, 2006; Miaczynska & Stenmark, 2008). Although each endocytic pathway was originally thought of as being distinct, it is now clear that they can overlap considerably and vesicles derived from CIDE can fuse with vesicles derived from the clathrin-dependent pathway (Doherty & McMahon, 2009).

Viruses can exploit CME and CIDE for entry into cells (Marsh & Helenius, 2006). Further, a number of viruses have been shown to utilize more than one pathway for internalization. For example, influenza virus has been shown to utilize both CME and a CIDE pathway for infection (Rust *et al.*, 2004) and SV40 can use at least two distinct lipid raft-mediated endocytic pathways for uptake (Damm *et al.*, 2005; Pelkmans *et al.*, 2001; Pelkmans *et al.*, 2002).

Currently, little is known of the mechanisms used by noroviruses to bind and enter cells. Recently, it was shown that feline calicivirus (FCV) uses junctional adhesion molecule A (JAM-A) as an attachment receptor (Makino *et al.*, 2006). In addition, FCV has been shown to bind to 2,6-sialic acid (Stuart & Brown, 2007), which could serve as a co-receptor for infection. Also, FCV is known to be internalised by CME as infection is inhibited by expression of dominant-negative mutants of proteins (Eps15 and Rab5) that are normally involved in clathrin-mediated endocytosis (Stuart & Brown, 2006).

MNV-1 replicates efficiently in macrophages and dendritic cells (Wobus *et al.*, 2004) and recently sialic acid was identified as a cellular receptor for MNV-1 on the

mouse macrophage cell line, RAW264.7 cells (Taube *et al.*, 2009). However, in contrast to FCV, a recent report (Perry *et al.*, 2009) showed that MNV-1 infection of RAW264.7 cells and primary DCs is pH-independent, suggesting that the entry pathway is clathrin independent. Here, we have investigated the cell entry mechanism used by MNV-1 to infect RAW264.7 cells. Our results suggest that MNV-1 entry can occur via a pathway that is clathrin- and caveolae-independent but requires dynamin and cholesterol.

Results

MNV-1 infection of RAW 264.7 cells is clathrin-independent

As FCV is closely related to MNV-1 and has been shown to utilize CME for entry into cultured cells, we determined if MNV-1 also utilizes this same pathway to infect RAW264.7 cells. Eps15 is a molecular scaffold protein which associates with both the AP-2 adaptor protein complex (Benmerah *et al.*, 1996; Benmerah *et al.*, 1995; Iannolo *et al.*, 1997) and epsin 1 (Chen *et al.*, 1998), and is required for CME of transferrin. RAW264.7 cells were transfected to express a dominant-negative (DN) form of Eps15 that is known to inhibit clathrin-mediated endocytosis (DN-Eps15 EΔ95/295; (Benmerah *et al.*, 1999), or a control form of Eps15 (DIIIΔ2) that lacks one of the AP-2 binding sites and does not interfere with the clathrin pathway. The transfected cells were identified by confocal microscopy via an eGFP tag on the Eps15 proteins (shown in green in **Figure 1**). At 12 h post-transfection, the cells were infected with MNV-1 at a low multiplicity of infection (MOI ~ 2), to favour virus uptake via the most efficient entry pathway. After 12 h, the cells were fixed and labelled using antisera to the viral NS7 polymerase protein to

identify infected cells. The Eps15-expressing cells (green) were scored for infection (red) and the number of infected cells in the DN-Eps15 expressing cell population normalised to the level of infection of the cells expressing the control protein (DIIIΔ2). This showed that expression of the DN Eps15 did not appear to inhibit MNV-1 infection (**Figure 1A)** suggesting that CME is not the entry route used by MNV-1 to infect RAW264.7 cells. To confirm that expression of DN-Eps15 inhibited CME, transfected RAW264.7 cells were also incubated with Alexa-labelled transferring, a commonly used marker for CME (Hinrichsen *et al.*, 2003). As expected, expression of the control Eps15 DIIIΔ2 protein had no effect on transferrin (red) uptake, whereas cells expressing the dominant negative Eps15 showed reduced transferrin uptake (**Figure 1B and 1C**).

To confirm that CME is not required for MNV-1 infection, RAW264.7 cells were transfected with siRNA targeted to the AP-2 adaptor complex. AP-2 is one of the major components of clathrin coat assembly and plays a central role in formation of clathrin coated pits (Mills, 2007). Following transfection, immunoblotting was performed to confirm a knock-down of AP-2 (**Figure 1E**). Transfection with AP-2 siRNA also inhibited transferrin uptake, confirming that CME was inhibited (**Figure 1D and 1G**). siRNA-transfected cells were also infected with MNV-1 and infection scored by confocal microscopy, as described above. Although AP-2 levels were greatly reduced and CME was inhibited, knockdown of AP-2 expression had no effect on MNV-1 infection (**Figure 1F).** Taken together, these results strongly suggest that MNV-1 does not use CME as the major entry route of RAW 264.7 cells.

Inhibition of endosomal acidification does not affect MNV-1 infection

A recent study has suggested that MNV-1 infection does not require endosome acidification (Perry *et al.*, 2009). To confirm this, we investigated the effect of concanamycin A on MNV-1 infection. Concanamycin A is a potent and specific inhibitor of the vacuolar proton ATPase (Huss *et al.*, 2002) and is commonly used to raise the pH within endosomes. RAW264.7 cells were treated with concanamycin A (or with DMSO as control) for 0.5 h prior to MNV-1 infection for 1 h. The cells were washed and incubated for a further 11 h, and infection quantified using the ELISPOT assay (**Figure 2A)** (Berryman *et al.*, 2005). Treatment of cells with concanamycin-A had no effect on MNV-1 infection (**Figure 2B**), confirming that MNV-1 infection does not require virus exposure to the low pH within acidic endosomes.

Depletion of cellular cholesterol inhibits MNV-1 endocytosis

Cholesterol depletion affects a number of endocytic pathways, including caveolin-dependent endocytosis (Pelkmans *et al.*, 2001; Smith *et al.*, 2003), as well as other lipid-raft mediated pathways ((Damm *et al.*, 2005; Vidricaire & Tremblay, 2007). MβCD depletes cholesterol from the plasma membrane and disrupts lipid rafts and endocytic pathways that involve these structures. RAW264.7 cells were pre-treated with MβCD (or DMSO) for 0.5 h and then infected with MNV-1 in the presence, or absence (no drug control) of the drug for 1 h. The virus inoculum and drug were removed by washing and infection continued at 37 ^{0}C for a further 11 h, before quantification using the ELISPOT assay. Treatment of cells with MβCD decreased MNV-1 infection by approximately 50% (**Figure 3A**). To confirm that the drug affected only an early step in infection, and not subsequent virus replication, the drug was also added immediately after, or 1.5 h after the

virus inoculum was removed. Under these conditions, no effect on infection was observed (**Figure 3A**), indicating that MβCD inhibited only the cell entry process and not subsequent steps in the replication cycle.

To ensure that MβCD did not inactivate the virus itself, virus was incubated with MβCD or DMSO (control) and residual infectivity measured by TCID50. This analysis showed that MβCD treatment had no effect on MNV-1 infectivity for RAW264.7 cells (data not shown). Addition of soluble cholesterol to RAW264.7 cells after MβCD treatment reversed the inhibitory effect of MβCD on infection (Figure 3C), further suggesting cholesterol is required for MNV-1 entry.

To confirm that MβCD treatment resulted in inhibition of lipid raft-dependent endocytosis, we analysed the effect of the drug on cholera toxin B (CTB) uptake. CTB is internalised in a lipid raft-dependent manner after binding to its receptor GM1 ganglioside (Fujinaga *et al.*, 2003). CTB internalisation was blocked when RAW264.7 cells were treated with MβCD, confirming that lipid raft-dependent endocytosis was inhibited (**Figure 3B**). Furthermore, as severe cholesterol depletion has been shown to also inhibit CME (Vela *et al.*, 2007), we confirmed that MβCD treatment did not inhibit uptake of Alexa-568 transferrin (data not shown). These data suggest that MNV-1 infection is cholesterol-sensitive and likely to be mediated by a lipid-raft dependent pathway.

Caveolin-1 is not expressed in RAW 264.7 cells

The above results show that MNV-1 infection is sensitive to cholesterol depletion and may therefore be mediated via lipid-rafts. Caveolae-mediated endocytosis is initiated

185 at lipid rafts and inhibited by cholesterol depletion. Therefore, we investigated the role of
186 caveolae in MNV-1 infection. Caveolae formation requires the caveolin (Morrow &
187 Parton, 2005), however a number of reports have shown that RAW264.7 cells lack
188 caveolin and therefore caveolae (Cameron *et al.*, 1997; Fra *et al.*, 1994; Gorodinsky &
189 Harris, 1995; Lyden *et al.*, 2002). In order to confirm the absence of caveolin-1 in our
190 RAW264.7 cells, we subjected RAW264.7 cell lysates to immunoblotting. **Figure 3D**
191 shows that caveolin was detected in HEK293 cells but not in RAW 264.7 cells (**Figure**
192 **3D**). This is entirely consistent with previous reports that RAW264.7 cells lack this
193 protein. Thus, the MNV-1 entry pathway in RAW264.7 cells is not dependent on
194 caveolae.
195
196 **MNV-1 endocytosis is dynamin-dependent**
197 Dynamin-2 is a GTPase that mediates vesicle fission from the plasma membrane
198 and is required for both clathrin- and caveolae-mediated endocytosis (Damke *et al.*, 1994;
199 Henley *et al.*, 1998; Oh *et al.*, 1998). To assess if dynamin is involved in MNV-1
200 infection, we used dynasore, a small-molecule inhibitor of dynamin (Macia *et al.*, 2006).
201 RAW264.7 cells were treated with dynasore (or DMSO) for 0.5 h, prior to MNV-1
202 infection. The virus inoculum was removed and the cells were incubated at 37^0C for a
203 further 11 h in the presence, or absence (control) of dynasore (as the effects of dynasore
204 are rapidly reversible). The cells were then fixed and infection quantified using the
205 ELISPOT assay. Treatment of RAW264.7 cells with dynasore inhibited infection by
206 85% (**Figure 4A**). Addition of the drug immediately after, or 1.5 h after the virus
207 inoculum was removed, had no effect on infection, suggesting that the drug only affected

entry and not a subsequent intracellular replication step. We also confirmed that dynasore did not inactivate virus in solution using the same approach as described for MβCD above (data not shown). As the drug remained present throughout the entire assay, we also assessed any cytotoxic effects on the cells. This analysis showed that only ~5% of cells displayed signs of cytotoxicity after 12 h treatment with dynasore (data not shown). In order to confirm that dynasore inhibited dynamin-dependent endocytosis, we analyzed the effect of the drug on uptake of Alexa-labelled transferrin. As expected, transferrin uptake was inhibited by dynasore (data not shown). These results suggest that dynamin is required for MNV-1 infection of RAW264.7 cells.

Microtubules are involved in MNV-1 infection

Nocodazole interferes with microtubule function and vesicular trafficking through the endosomal pathway (D'Hondt *et al.*, 2000). RAW264.7 cells were treated with nocodazole (or DMSO) for 0.5 h prior to MNV-1 infection and infection was quantified using the ELISPOT assay. Nocodazole treatment inhibited MNV-1 infection by 40-50 % (**Figure 4B**), suggesting that an early stage of MNV-1 infection requires intact microtubules. Addition of the drug immediately after the virus inoculum was removed also had a small inhibitory effect on infection, suggesting that microtubules may also be involved in trafficking of the virus post-entry. At the concentrations used, nocodazole was shown to disrupt the microtubules, as revealed by indirect immunofluorescence confocal microscopy using anti-tubulin antisera (data not shown).

Blocking macropinocytosis enhances MNV-1 infection

231 Macropinocytosis (MPC) is used by a number of viruses for infectious entry
232 (Mercer & Helenius, 2008). To determine if MPC is active in RAW264.7 cells, we used
233 uptake of Alexa-labelled dextran (Dharmawardhane et al., 2000). **Figure 5B** shows that
234 dextran was internalised by RAW264.7 cells, indicating that MPC was active. Next, we
235 investigated the effect of EIPA on infection. EIPA is an analogue of amiloride and
236 inhibits Na^+/H^+ exchangers and MPC without affecting other endocytic pathways such as
237 CME, or cavoelae-mediated endocytosis (West *et al.*, 1989). We first confirmed that
238 EIPA blocked MPC in RAW264.7 cells by showing that treatment of the cells with this
239 drug inhibited dextran uptake (**Figure 5B**). However, we found that EIPA had an
240 unexpected effect on MNV-1 infection, as treatment of cells with EIPA resulted in
241 enhanced MNV-1 infection (by 47% at 25 μM and 67% at 50 μM) (**Figure 5A**). Actin
242 filaments are important for MPC, therefore we investigated the effect of actin disruption
243 on MNV-1 infection using cytochalasin-D, which prevents actin polymerization and
244 disrupts the actin cytoskeleton (Brenner & Korn, 1980). Consistent with the effect of
245 EIPA, cytochalasin-D treatment of RAW264.7 cells also enhanced MNV-1 infection
246 (**Figure 5C**) by about 60%. At the concentrations used, cytochalasin D was shown to
247 disrupt actin filaments, as revealed by indirect immunofluorescence confocal microscopy
248 using Alexa-conjugated phalloidin (**Figure 5D**).
249
250 **Depletion of flotillin-1 does not inhibit MNV-1 internalisation**
251 We also analysed the effect of flotillin-1 depletion on MNV-1 infection. Flotillin-
252 1 is associated with lipid rafts and was recently identified as a component of a novel
253 CIDE pathway (Glebov *et al.*, 2006; Lang *et al.*, 1998; Volonte *et al.*, 1999). RAW264.7

cells were transfected with siRNA against flotillin-1 and inhibition of flotillin-1 expression confirmed by immunoblotting (**Figure 6A**); no effect on flotillin-1 expression was observed when compared to cells transfected with a control siRNA targeted to GFP. This knock-down of flotillin-1 had no effect on MNV-1 infection (**Figure 6B**), suggesting that the flotillin-1-dependent pathway is not involved in MNV-1 entry.

Discussion

Viruses have been shown to utilize a number of different endocytic pathways to enter and infect cells. CME would appear to be the most commonly used but it is increasingly clear that a number of CIDE pathways are also used by several different viruses. It has recently been shown that entry of MNV-1 into RAW264.7 cells is pH-independent (Perry *et al.*, 2009). In this study we have further examined the entry route used by MNV-1 to infect RAW264.7 cells. Initially, we investigated if infection by MNV-1 is dependent on CME, since FCV (which is closely related to MNV-1) is internalised via this pathway (Stuart & Brown, 2006). Our experiments show that dominant negative Eps-15 and AP-2 knock-down inhibited transferrin uptake but had no effect on MNV-1 infection, strongly suggesting that the mechanism of MNV-1 entry is clathrin-independent. Similarly, concanamycin A treatment confirmed that a low pH within endosomes is not required for MNV-1 infection, further supporting the conclusion that a clathrin-independent pathway is most likely required for MNV-1 entry.

A number of CIDE pathways originate from lipid rafts. These pathways require cholesterol and can be inhibited by the cholesterol-depleting agent MβCD. We found that treatment of RAW264.7 cells with MβCD inhibited MNV-1 infection, but only when the

277 drug was added during virus entry and not when added after virus uptake. Repletion of
278 cholesterol after MβCD treatment restored infection, further suggesting that cholesterol is
279 required for MNV-1 infection.

280 Our data suggests that MNV-1 entry into RAW264.7 cells is cholesterol and
281 hence lipid raft-dependent. Caveolae-dependent endocytosis also requires intact lipid-
282 rafts and hence, is normally inhibited by cholesterol depletion (Murata *et al.*, 1995).
283 Caveolin is a key component of caveolae (Morrow & Parton, 2005); however, a number
284 of previous studies have shown that RAW264.7 cells lack caveolin (Cameron *et al.*,
285 1997; Fra *et al.*, 1994; Gorodinsky & Harris, 1995; Lyden *et al.*, 2002). and we have
286 confirmed these observations in our RAW264.7 cells. These data do not rule out the
287 possibility that MNV-1 infection may occur through a caveolae-dependent pathway in
288 other cell types which express caveolin. The recently described flotillin-dependent
289 pathway is also raft-associated (Glebov *et al.*, 2006) and may be inhibited by cholesterol
290 depletion; however, our results showed that flotillin-1 depletion had no effect on MNV-1
291 infection, suggesting that this pathway is also not used for MNV-1 infection.

292 The role of dynamin in both CME and caveolae-dependent endocytosis is well-
293 established, whereas its role in other endocytic pathways is less clear (Marsh & Helenius,
294 2006; Miaczynska & Stenmark, 2008). Here we show that inhibition of dynamin using
295 dynasore decreased MNV-1 infection of RAW264.7 cells, but only when added at the
296 entry stage of infection, indicating that MNV-1 entry is dynamin-dependent.

297 Treatment of RAW.264.7 cells with nocodazole (which disrupts microtubules)
298 also inhibited MNV-1 infection. However, at this stage we cannot be certain if
299 microtubules are required for entry or post-entry virus trafficking as the drug also

inhibited infection when added immediately after the virus inoculum was removed and further studies are required to understand the precise role for microtubules during virus entry.

Recently, a number of viruses have been shown to use MPC, or MPC-like entry pathways for infection (reviewed in Mercer and Helenius, 2009). MPC is especially active in specialised antigen-presenting cells, such as macrophages and dendritic cells. Therefore, we also investigated a role for MPC in MNV-1 infection. We established that MPC was active in RAW264.7 cells but surprisingly, inhibition of MPC, by either EIPA or cytochalasin D, resulted in an increase in MNV-1 infection. At present we do not know why inhibiting MPC should lead to an increase in infection. A possible explanation is that MPC is responsible for a large proportion of fluid-phase uptake and inhibition of MPC could result in up-regulation of other endocytic pathways (by way of compensation) that could then be used for MNV-1 uptake. Alternatively, it is possible that a proportion of virus enters RAW264.7 cells by MPC and is delivered to lysosomes for destruction. If this is the case then inhibition of MPC may lead to enhanced infection. However, further studies are needed to understand this phenomenon.

In conclusion, we have presented evidence that infection of RAW264.7 cells by MNV-1 is mediated by a clathrin-, caveolae-, flotillin- and pH-independent pathway that requires intact lipid-rafts, dynamin and microtubules. Together these studies suggest that different members of the calicivirus family may utilize different cell entry pathways for infection.

Methods

323

324 **Cell culture and viruses**

325 RAW264.7 and HEK293 cells were cultivated in Dulbecco's modified Eagle's
326 medium (DMEM) and modified Eagle's medium (MEM), respectively, supplemented
327 with 10% foetal bovine serum, non-essential amino acids (1 %), penicillin (100 U/ml)
328 and streptomycin (100 mg/ml; Gibco-BRL) at 37 °C with 5% CO_2. MNV-1 (strain CW.1)
329 was the gift of Prof. Herbert Virgin (Washington University, St. Louis, MO) and was
330 propagated in RAW264.7 cells. The virus titre was determined by TCID50 on RAW264.7
331 cells.

332

333 **Antibodies and reagents**

334 The anti-α-tubulin antisera (DM1A) was from Sigma. Anti-flotillin-1 antisera
335 (clone 18) was from BD Biosciences. Anti-adaptin-2 (AP-2) monoclonal antibody (sc-
336 55497) and polyclonal anti-caveolin-1 sera (sc-894) were from Santa Cruz Biotechnology.
337 The anti-GAPDH monoclonal antibody (6C5) was from Ambion. The anti-MNV NS7
338 polymerase polyclonal sera was a gift of Dr Ian Goodfellow (Imperial College, London,
339 UK). Alexa-568 transferrin, alexa-555 cholera toxin B and alexa-555 dextran were all
340 from Invitrogen, as were the Alexa-Fluor-conjugated secondary antibodies. 5-(N-Ethyl-
341 N-isopropyl) amiloride (EIPA), concanamycin A, cytochalasin D, nocodazole, dynasore,
342 and methyl-β-cyclodextrin (MβCD) and water soluble cholesterol (C4951) were from
343 Sigma. Stock solutions of concanamycin A, EIPA, cytochalasin D, dynasore and
344 nococodazole were prepared in dimethyl sulfoxide (DMSO). A stock solution of MβCD

345 was prepared in DMEM. Where appropriate, an equivalent dilution of DMSO was
346 included as the control treatment.
347
348 **Quantification of virus infection assays**
349 To quantify MNV-1 infection, a modification of an enzyme-linked immunospot
350 (ELISPOT) assay was used (Berryman *et al.*, 2005). Briefly, $3x10^4$ cells were seeded per
351 well in 96-well tissue culture plates and grown overnight until approximately 80%
352 confluent. The cells were incubated for 1 h at 37°C with MNV-1 at a multiplicity of
353 infection (MOI) of ~2 pfu/cell. The cells were washed to remove excess virus and
354 incubated in growth media at 37°C for a further 11 h. Cells were fixed by the addition of
355 cold 4% paraformaldehyde (PFA; Sigma) in phosphate-buffered saline (PBS) for 1 h. The
356 cells were then permeabilized with 0.1% Triton X-100 in PBS for 15 min. Following
357 incubation for 0.5 h in blocking buffer (0.5% BSA in PBS), the cells were incubated with
358 anti-MNV NS7 polymerase antisera (1:1500) for 1 h at RT. The cells were washed again
359 and incubated with a biotinylated goat anti-rabbit IgG antisera (1:400; Southern
360 Biotechnologies) followed by a streptavidin-conjugated alkaline phosphatase (1:1000;
361 Caltag Laboratories) in blocking buffer for 1 h at RT. The alkaline phosphatase substrate
362 (Bio-Rad) was added for 10 min, according to the manufacturer's instructions. The
363 infected cells stained dark blue and were quantified using an ELISPOT plate reader
364 (Zeiss KS ELIspot). Nonspecific labelling was determined by performing the assay on
365 mock-infected cells.
366 To determine the effect of pharmacological inhibitors of endocytosis on MNV-1
367 infection, cells were (i) pre-treated with the drug for 0.5 h prior to infection with MNV-1

368 for 1h, also in the presence of the drug; or (ii) treated with the drug for 1.5 h immediately
369 after the virus inoculum was removed, or (iii) the drug was added 1.5 h after the virus
370 inoculum was removed. In the case of the dynasore, the drug was present throughout the
371 assay.

372 To control for effects of the inhibitors on virus in solution, virus was incubated
373 with 7.5 mM of MβCD or 50 μM dynasore for 15 mins at RT. Control virus was
374 incubated with DMSO alone. Drug treated and control viruses were then titrated by
375 TCID50 assay as described previously (Bailey *et al*, 2008).

376 Following MβCD treatment, cells were treated with 400 μg/ml water soluble
377 cholesterol for 15 mins at RT, before removing the medium, to replete the cholesterol in
378 the plasma membrane. Cells were subsequently infected with MNV-1 as described above
379 and virus infection quantified by confocal microscopy.

380

381 **Transfections**

382 Transient transfection of RAW264.7 cells with plasmids expressing dominant
383 negative or control Eps15 (gift from Alexandre Benmerah, Université Paris Descartes,
384 Paris, France) was performed using Fugene HD (Roche) and 2 μg DNA per well (24 well
385 plate), according to the manufacturer's instructions. siRNAs targeted against flotillin-1
386 (5' GCUACACUUUGAAGGAUAU) or adaptin-2 (AP-2; 5'
387 GACCCACAUUGAUACAGUU; Eurogentec) were transfected into RAW264.7 cells as
388 follows; cells ($3x10^4$) were seeded on 13-mm glass coverslips (BDH) and 0.1 μM of the
389 siRNA, or a control siRNA duplex targeted against GFP, was added per well. Forty-eight
390 hours post-transfection, the cells were infected with MNV-1 (MOI ~ 2) for 1 h at 37^{o}C.

391 Excess virus was removed and the cells incubated for a further 11 h. The cells were
392 washed with PBS, fixed with cold 4% PFA for 1 h and processed for confocal
393 microscopy using the anti-MNV NS7 polymerase antisera (1:1500) as described below.
394 To confirm siRNA-mediated knockdown of the targeted proteins, cell extracts were
395 subjected to SDS-PAGE and immunoblotting using anti-flotillin-1 and anti-AP-2 antisera.
396 Membranes were re-probed with anti-GAPDH antisera as a loading control.
397
398 **Immunofluorescence confocal microscopy**
399 RAW264.7 cells (3 x 10^4cells/well) were seeded onto 13-mm glass coverslips
400 (BDH) and infected with MNV-1 in the presence/absence of endocytosis inhibitors, as
401 described above. Cells were washed with PBS, fixed with cold 4% PFA for 1 h, and
402 permeabilized for 15 min with 0.1% Triton X-100 in blocking buffer. The cells were
403 incubated with primary antibody for 1 h at RT, washed and incubated with the
404 appropriate Alexa-conjugated secondary antibody in blocking buffer for 1 h at RT. After
405 washing, the cells were incubated with TO-PRO-3 iodide (Invitrogen) for 10 min at RT to
406 stain the cell nuclei. The cells were mounted onto slides using Vectashield mounting
407 medium (Vector Labs) and sealed. Uptake of Alexa-labelled ligands (Dextran 0.5μg/ml,
408 Cholera toxin B 10μg/ml and Transferrin 15 μg/ml) was carried out for the times
409 indicated in the figures before fixing the cells and processing for microscopy as described
410 above. If labelling with antibodies was not required, cells were processed without
411 permeabilization. Microscopy was performed using a ZEISS 510Meta, equipped with a
412 63x 1.4 NA Zeiss apochomat objective. All data were collected sequentially, to eliminate
413 cross talk between the fluorescent dyes, using the same microscope settings.

414

415 **Immunoblotting**

416 Cell pellets were resuspended in RIPA buffer (50mM Tris-cl pH 7.4,150mM
417 NaCl, 1% NP40, 0.25% Na-deoxycholate, 1mM PMSF) and centrifuged at 14,000 rpm
418 for 5 min at 4 ^{0}C. Lysates were subjected to SDS-PAGE (12%) and proteins transferred
419 to nitrocellulose membranes. Membranes were probed with the indicated primary
420 antibodies followed by horseradish peroxidase (HRP)-conjugated species-specific
421 secondary antibodies (1:2000; Dako). Proteins were visualised by chemiluminescence
422 (Pierce).

423

424 **Statistical analysis**

425 All studies were performed independently at least three times. The mean and
426 standard error of the mean are shown. GraphPad prism 5 (GraphPad) was used to
427 perform the statistical analysis. One way Anova with Dunnett post-hoc test was used to
428 evaluate the differences between treatments. Significance was determined by a P value of
429 < 0.05, and significance is indicated in each figure.

430

431 **Acknowledgements**

432 We thank Prof. Herbert Virgin for MNV-1 and Dr Stephen Berryman for technical help
433 with the Elispot assay.

434

435 **Figure legends**

436

Figure 1: MNV-1 entry is clathrin-independent

(A) RAW264.7 cells were transiently transfected to express control Eps15 (DIIIΔ2) or dominant negative Eps-15 (ED95/295 Eps15) as fusions with eGFP. Transfected cells were identified by eGFP expression. At 12 h post-transfection, cells were infected with MNV-1 (MOI ~2) for 12 h. Infected cells were quantified by confocal microscopy using an antibody to the viral NS7 polymerase protein. Results are shown as the level of infection of the DN Eps15-expressing cells normalized to the level of infection of the cells expressing the control protein. The mean ±SE of 3 independent experiments is shown. (B) RAW264.7 cells were transfected to express the control or DN-Eps15 as described in panel A. At 12 h post-transfection, Alexa-568-conjugated transferrin (red) was internalized for 10 min and then chased for 20 min in the absence of transferrin. The nuclei were stained with TO-PRO-3 iodide and are shown in blue. Scale bar 10 μm. (C) Transferrin internalization was quantified by confocal microscopy. Results are shown as the level of transferrin uptake by the DN Eps15-expressing cells normalized to the level of uptake by the cells expressing the control protein. The mean ±SE of 3 independent experiments is shown. (D) RAW264.7 cells were transfected with siRNA targeted against AP-2 or a control siRNA against GFP. At 48 h post-transfection, Alexa-568-conjugated transferrin (red) was internalized for 10 min and then chased for 20 min in the absence of transferrin. The nuclei were stained with TO-PRO-3 iodide and are shown in blue. Scale bar 10 μm. (E) RAW264.7 cells were transfected with siRNA targeted against AP-2 or siRNA against GFP and at 48 h post-transfection, cell lysates were analyzed by SDS-PAGE and immunoblotting with AP-2 and GAPDH antisera. (F) 48 h post-transfection with the AP-2 and GFP siRNAs, cells were infected with MNV-1 (MOI ~ 2) for 12 h and

infected cells quantified as above. Results are shown as the level of infection of the AP2 siRNA-transfected cells normalized to the level of infection of the cells transfected with the control GFP siRNA. The mean ±SE from 3 independent experiments is shown. (G) The siRNA-transfected cells were quantified for transferrin internalization by confocal microscopy. Results are shown as the level of transferrin uptake by the AP-2 siRNA transfected cells normalized to the level of uptake by the cells transfected with the control siRNA. The mean ±SE of 3 independent experiments is shown.

Figure 2: MNV-1 entry is not pH-dependent

(A) RAW264.7 cells were infected with MNV-1 (MOI ~2), or mock-infected, for 1 h at 37°C. The cells were washed and incubated in culture medium for a further 11 h and then fixed and permeabilized. Infected cells were quantified using the ELISPOT assay. Panel (i) shows a mock-infected cell monolayer. Panel (ii) shows an infected cell monolayer. (B) RAW264.7 cells were pre-treated with different concentrations of concanamycin A for 0.5 h prior to infection with MNV-1 (MOI ~ 2) for 1 h in the presence of the drug. Control-treated cells were treated with an equivalent dilution of DMSO. The cells were then washed and incubated in culture medium for a further 11 h, and infection quantified using the ELISPOT assay. Results are shown as the level of infection of the drug treated cells normalized to the level of infection in the absence of the drug. The mean ±SE from 3 independent experiments is shown.

Figure 3: MNV-1 entry is cholesterol-dependent

(A) RAW264.7 cells were pre-treated with different concentrations of MβCD prior to infection with MNV-1 (MOI ~ 2) for 1 h in the presence (or absence) of the drug. Virus and drug were removed and infection quantified at 12 h.p.i using the ELISPOT assay. To control for effects on intracellular virus replication, the drug was added for 1.5 h either immediately after the virus inoculum had been removed, or 1.5 h after the virus inoculum was removed. The results are shown as the level of infection of the drug-treated cells normalized to the level of infection in the absence of the drug The mean ±SE from 3 independent experiments is shown. *p<0.05, **p<.0.01 (B) RAW264.7 cells were treated (or control treated) with 7.5 mM MβCD for 0.5 h, prior to the internalization of Alexa-555-conjugated CTB (shown in green) for 0.5 h. The nuclei were stained with TO-PRO-3 iodide (blue). Scale bars = 10 μm. (C) For repletion of cholesterol following MβCD treatment, cells were treated with 400ug/ml water soluble cholesterol prior to infection, as above. Results shown are representative of two independent experiments. (D) RAW264.7 cell and HEK293 cell lysates were subjected to SDS-PAGE and immunoblotting with anti-caveolin-1 and anti-GAPDH antisera.

Figure 4: MNV-1 entry is dynamin-dependent and involves microtubules

(A) RAW264.7 cells were treated with dynasore (or DMSO) for 0.5 h prior to infection with MNV-1 (MOI ~2) for 12h, with the drug remaining present throughout the assay. Infected cells were quantified by ELISPOT assay as described in Figure 2. To control for post-entry effects on virus replication, the drug was added immediately after, or 1.5 h after, the virus inoculum was removed. The results are shown as the level of infection of the drug-treated cells normalized to the level of infection in the absence of the drug. The

505 mean ±SE from 3 independent experiments is shown. ***p<0.001. (B) RAW264.7 cells
506 were pretreated with nocodazole (or DMSO) prior to infection with MNV-1 (MOI of ~2)
507 for 12 h. Infection was quantified by ELIspot assay. The drug was also added post entry
508 as described above. The results are shown as the level of infection of the drug-treated
509 cells normalized to the level of infection in the absence of the drug. Shown is the mean
510 ±SE from 3 experiments. *p<0.05, **p<, ***p<0.001.
511
512 **Figure 5: Role of macropinocytosis and F-actin in MNV-1 infection**
513 (A) RAW264.7 cells were pretreated with 25 µM and 50 µM EIPA prior to infection with
514 MNV-1 (MOI of ~2) for 12 h. Infection was quantified by ELISPOT assay as described
515 in Figure 2. The results are shown as the level of infection of the drug treated cells
516 normalized to the level of infection of the mock treated cells. Shown is the mean ±SE
517 from 3 experiments. *p<0.05. (B) RAW264.7 cells were pretreated with 50 µM EIPA for
518 0.5 h and incubated with 0.5 µg/ml Alexa-labelled dextran (red) for 0.5 h. The
519 intracellular distribution of fluorescent dextran in EIPA-treated samples was compared to
520 that in the untreated cells. The nuclei were stained with TO-PRO-3 iodide (blue). Scale
521 bars = 10 µm**.** (C) RAW264.7 cells were pretreated with 2, 4 or 8 µM cytochalasin D
522 prior to infection with MNV-1 (MOI of ~2). Infection was quantified by ELISPOT.
523 Shown is the mean ±SE from 3 experiments. (D) RAW264.7 cells were pretreated with 4
524 µM cytochalasin D and the actin microfilaments stained with phalloidin. Nuclei were
525 stained as described above. Scale bars = 10 µm.
526
527 **Figure 6: Flotillin-1 is not involved in MNV-1 infection**

RAW264.7 cells were transfected with siRNA targeted against flotillin-1 or GFP (control). (A) 48 h post-transfection, cell lysates were prepared and analyzed by immunoblotting with anti-flotillin-1 and anti-GAPDH antisera. (B) 48 h post-transfection, cells were infected with MNV-1 (MOI ~ 2), virus inoculum was removed after 1h and the infection continued for a further 11 h. The cells were fixed and permeabilized and infected cells detected using anti-MNV-1 NS7 polymerase antisera and an Alexa-543 goat anti-rabbit IgG antibody before visualization by confocal microscopy. Results are shown as the level of infection of the flotillin-1 siRNA transfected cells (Flot-1) normalized to the level of infection of the cells transfected with the GFP siRNA. The mean ±SE from 3 independent experiments is shown.

References

Bailey, D., Thackray, L. B. & Goodfellow I. G. (2008), A Single Amino Acid Substitution in the Murine Norovirus Capsid Protein Is Sufficient for Attenuation In Vivo *Journal of Virology* **82 (Pt 15),** 7725–7728.

Benmerah, A., Bayrou, M., Cerf-Bensussan, N. & Dautry-Varsat, A. (1999). Inhibition of clathrin-coated pit assembly by an Eps15 mutant. *Journal of cell science* **112 (Pt 9)**, 1303-1311.

Benmerah, A., Begue, B., Dautry-Varsat, A. & Cerf-Bensussan, N. (1996). The ear of alpha-adaptin interacts with the COOH-terminal domain of the Eps 15 protein. *The Journal of biological chemistry* **271**, 12111-12116.

Benmerah, A., Gagnon, J., Begue, B., Megarbane, B., Dautry-Varsat, A. & Cerf-Bensussan, N. (1995). The tyrosine kinase substrate eps15 is constitutively associated with the plasma membrane adaptor AP-2. *The Journal of cell biology* **131**, 1831-1838.

Berryman, S., Clark, S., Monaghan, P. & Jackson, T. (2005). Early events in integrin alphavbeta6-mediated cell entry of foot-and-mouth disease virus. *Journal of virology* **79**, 8519-8534.

Brenner, S. L. & Korn, E. D. (1980). The effects of cytochalasins on actin polymerization and actin ATPase provide insights into the mechanism of polymerization. *The Journal of biological chemistry* **255**, 841-844.

Cameron, P. L., Ruffin, J. W., Bollag, R., Rasmussen, H. & Cameron, R. S. (1997). Identification of caveolin and caveolin-related proteins in the brain. *J Neurosci* **17**, 9520-9535.

Chen, H., Fre, S., Slepnev, V. I., Capua, M. R., Takei, K., Butler, M. H., Di Fiore, P. P. & De Camilli, P. (1998). Epsin is an EH-domain-binding protein implicated in clathrin-mediated endocytosis. *Nature* **394**, 793-797.

D'Hondt, K., Heese-Peck, A. & Riezman, H. (2000). Protein and lipid requirements for endocytosis. *Annual review of genetics* **34**, 255-295.

Damke, H., Baba, T., Warnock, D. E. & Schmid, S. L. (1994). Induction of mutant dynamin specifically blocks endocytic coated vesicle formation. *The Journal of cell biology* **127**, 915-934.

Damm, E. M., Pelkmans, L., Kartenbeck, J., Mezzacasa, A., Kurzchalia, T. & Helenius, A. (2005). Clathrin- and caveolin-1-independent endocytosis: entry of simian virus 40 into cells devoid of caveolae. *The Journal of cell biology* **168**, 477-488.

Dharmawardhane, S., Schurmann, A., Sells, M. A., Chernoff, J., Schmid, S. L. & Bokoch, G. M. (2000). Regulation of macropinocytosis by p21-activated kinase-1. *Molecular biology of the cell* **11**, 3341-3352.

Doherty, G. J. & McMahon, H. T. (2009). Mechanisms of endocytosis. *Annual review of biochemistry* **78**, 857-902.

Fra, A. M., Williamson, E., Simons, K. & Parton, R. G. (1994). Detergent-insoluble glycolipid microdomains in lymphocytes in the absence of caveolae. *The Journal of biological chemistry* **269**, 30745-30748.

583 **Fujinaga, Y., Wolf, A. A., Rodighiero, C., Wheeler, H., Tsai, B., Allen, L., Jobling,**
584 **M. G., Rapoport, T., Holmes, R. K. & Lencer, W. I. (2003).** Gangliosides that
585 associate with lipid rafts mediate transport of cholera and related toxins from the
586 plasma membrane to endoplasmic reticulm. *Molecular biology of the cell* **14**,
587 4783-4793.
588 **Glebov, O. O., Bright, N. A. & Nichols, B. J. (2006).** Flotillin-1 defines a clathrin-
589 independent endocytic pathway in mammalian cells. *Nature cell biology* **8**, 46-54.
590 **Gorodinsky, A. & Harris, D. A. (1995).** Glycolipid-anchored proteins in neuroblastoma
591 cells form detergent-resistant complexes without caveolin. *The Journal of cell*
592 *biology* **129**, 619-627.
593 **Henley, J. R., Krueger, E. W., Oswald, B. J. & McNiven, M. A. (1998).** Dynamin-
594 mediated internalization of caveolae. *The Journal of cell biology* **141**, 85-99.
595 **Hinrichsen, L., Harborth, J., Andrees, L., Weber, K. & Ungewickell, E. J. (2003).**
596 Effect of clathrin heavy chain- and alpha-adaptin-specific small inhibitory RNAs
597 on endocytic accessory proteins and receptor trafficking in HeLa cells. *The*
598 *Journal of biological chemistry* **278**, 45160-45170.
599 **Hsu, C. C., Riley, L. K., Wills, H. M. & Livingston, R. S. (2006).** Persistent infection
600 with and serologic cross-reactivity of three novel murine noroviruses.
601 *Comparative medicine* **56**, 247-251.
602 **Huss, M., Ingenhorst, G., Konig, S., Gassel, M., Drose, S., Zeeck, A., Altendorf, K. &**
603 **Wieczorek, H. (2002).** Concanamycin A, the specific inhibitor of V-ATPases,
604 binds to the V(o) subunit c. *The Journal of biological chemistry* **277**, 40544-
605 40548.
606 **Iannolo, G., Salcini, A. E., Gaidarov, I., Goodman, O. B., Jr., Baulida, J., Carpenter,**
607 **G., Pelicci, P. G., Di Fiore, P. P. & Keen, J. H. (1997).** Mapping of the
608 molecular determinants involved in the interaction between eps15 and AP-2.
609 *Cancer research* **57**, 240-245.
610 **Karst, S. M., Wobus, C. E., Lay, M., Davidson, J. & Virgin, H. W. t. (2003).** STAT1-
611 dependent innate immunity to a Norwalk-like virus. *Science (New York, NY* **299**,
612 1575-1578.
613 **Lang, D. M., Lommel, S., Jung, M., Ankerhold, R., Petrausch, B., Laessing, U.,**
614 **Wiechers, M. F., Plattner, H. & Stuermer, C. A. (1998).** Identification of
615 reggie-1 and reggie-2 as plasmamembrane-associated proteins which cocluster
616 with activated GPI-anchored cell adhesion molecules in non-caveolar
617 micropatches in neurons. *Journal of neurobiology* **37**, 502-523.
618 **Lopman, B. A., Reacher, M., Gallimore, C., Adak, G. K., Gray, J. J. & Brown, D. W.**
619 **(2003).** A summertime peak of "winter vomiting disease": surveillance of
620 noroviruses in England and Wales, 1995 to 2002. *BMC public health* **3**, 13.
621 **Lyden, T. W., Anderson, C. L. & Robinson, J. M. (2002).** The endothelium but not the
622 syncytiotrophoblast of human placenta expresses caveolae. *Placenta* **23**, 640-652.
623 **Macia, E., Ehrlich, M., Massol, R., Boucrot, E., Brunner, C. & Kirchhausen, T.**
624 **(2006).** Dynasore, a cell-permeable inhibitor of dynamin. *Developmental cell* **10**,
625 839-850.
626 **Makino, A., Shimojima, M., Miyazawa, T., Kato, K., Tohya, Y. & Akashi, H. (2006).**
627 Junctional adhesion molecule 1 is a functional receptor for feline calicivirus.
628 *Journal of virology* **80**, 4482-4490.

Marsh, M. & Helenius, A. (2006). Virus entry: open sesame. *Cell* **124**, 729-740.
Mercer, J. & Helenius, A. (2008). Vaccinia virus uses macropinocytosis and apoptotic mimicry to enter host cells. *Science (New York, NY* **320**, 531-535.
Miaczynska, M. & Stenmark, H. (2008). Mechanisms and functions of endocytosis. *The Journal of cell biology* **180**, 7-11.
Mills, I. G. (2007). The interplay between clathrin-coated vesicles and cell signalling. *Seminars in cell & developmental biology* **18**, 459-470.
Morrow, I. C. & Parton, R. G. (2005). Flotillins and the PHB domain protein family: rafts, worms and anaesthetics. *Traffic (Copenhagen, Denmark)* **6**, 725-740.
Muller, B., Klemm, U., Mas Marques, A. & Schreier, E. (2007). Genetic diversity and recombination of murine noroviruses in immunocompromised mice. *Archives of virology* **152**, 1709-1719.
Murata, M., Peranen, J., Schreiner, R., Wieland, F., Kurzchalia, T. V. & Simons, K. (1995). VIP21/caveolin is a cholesterol-binding protein. *Proceedings of the National Academy of Sciences of the United States of America* **92**, 10339-10343.
Oh, P., McIntosh, D. P. & Schnitzer, J. E. (1998). Dynamin at the neck of caveolae mediates their budding to form transport vesicles by GTP-driven fission from the plasma membrane of endothelium. *The Journal of cell biology* **141**, 101-114.
Pelkmans, L., Kartenbeck, J. & Helenius, A. (2001). Caveolar endocytosis of simian virus 40 reveals a new two-step vesicular-transport pathway to the ER. *Nature cell biology* **3**, 473-483.
Pelkmans, L., Puntener, D. & Helenius, A. (2002). Local actin polymerization and dynamin recruitment in SV40-induced internalization of caveolae. *Science (New York, NY* **296**, 535-539.
Perry, J. W., Taube, S. & Wobus, C. E. (2009). Murine norovirus-1 entry into permissive macrophages and dendritic cells is pH-independent. *Virus research* **143**, 125-129.
Rust, M., Lakadamyali, M., Zhang, F. & Zhuang, X. (2004). Assembly of endocytic machinerz around individual influenza viruses during viral entry. *Nature Structural and Molecular Biology* **11**, 567-573.
Smith, A. E., Lilie, H. & Helenius, A. (2003). Ganglioside-dependent cell attachment and endocytosis of murine polyomavirus-like particles. *FEBS letters* **555**, 199-203.
Sosnovtsev, S. V., Belliot, G., Chang, K. O., Prikhodko, V. G., Thackray, L. B., Wobus, C. E., Karst, S. M., Virgin, H. W. & Green, K. Y. (2006). Cleavage map and proteolytic processing of the murine norovirus nonstructural polyprotein in infected cells. *Journal of virology* **80**, 7816-7831.
Stuart, A. D. & Brown, T. D. (2006). Entry of feline calicivirus is dependent on clathrin-mediated endocytosis and acidification in endosomes. *Journal of virology* **80**, 7500-7509.
Stuart, A. D. & Brown, T. D. (2007). Alpha2,6-linked sialic acid acts as a receptor for Feline calicivirus. *The Journal of general virology* **88**, 177-186.
Taube, S., Perry, J. W., Yetming, K., Patel, S. P., Auble, H., Shu, L., Nawar, H. F., Lee, C. H., Connell, T. D., Shayman, J. A. & Wobus, C. E. (2009). Ganglioside-linked terminal sialic acid moieties on murine macrophages function as attachment receptors for Murine Noroviruses (MNV). *Journal of virology*.

Thackray, L. B., Wobus, C. E., Chachu, K. A., Liu, B., Alegre, E. R., Henderson, K. S., Kelley, S. T. & Virgin, H. W. t. (2007). Murine noroviruses comprising a single genogroup exhibit biological diversity despite limited sequence divergence. *Journal of virology* **81**, 10460-10473.

Vela, E. M., Zhang, L., Colpitts, T. M., Davey, R. A. & Aronson, J. F. (2007). Arenavirus entry occurs through a cholesterol-dependent, non-caveolar, clathrin-mediated endocytic mechanism. *Virology* **369**, 1-11.

Vidricaire, G. & Tremblay, M. J. (2007). A clathrin, caveolae, and dynamin-independent endocytic pathway requiring free membrane cholesterol drives HIV-1 internalization and infection in polarized trophoblastic cells. *Journal of molecular biology* **368**, 1267-1283.

Volonte, D., Galbiati, F., Li, S., Nishiyama, K., Okamoto, T. & Lisanti, M. P. (1999). Flotillins/cavatellins are differentially expressed in cells and tissues and form a hetero-oligomeric complex with caveolins in vivo. Characterization and epitope-mapping of a novel flotillin-1 monoclonal antibody probe. *The Journal of biological chemistry* **274**, 12702-12709.

West, M. A., Bretscher, M. S. & Watts, C. (1989). Distinct endocytotic pathways in epidermal growth factor-stimulated human carcinoma A431 cells. *The Journal of cell biology* **109**, 2731-2739.

Wobus, C. E., Karst, S. M., Thackray, L. B., Chang, K. O., Sosnovtsev, S. V., Belliot, G., Krug, A., Mackenzie, J. M., Green, K. Y. & Virgin, H. W. (2004). Replication of Norovirus in cell culture reveals a tropism for dendritic cells and macrophages. *PLoS biology* **2**, e432.

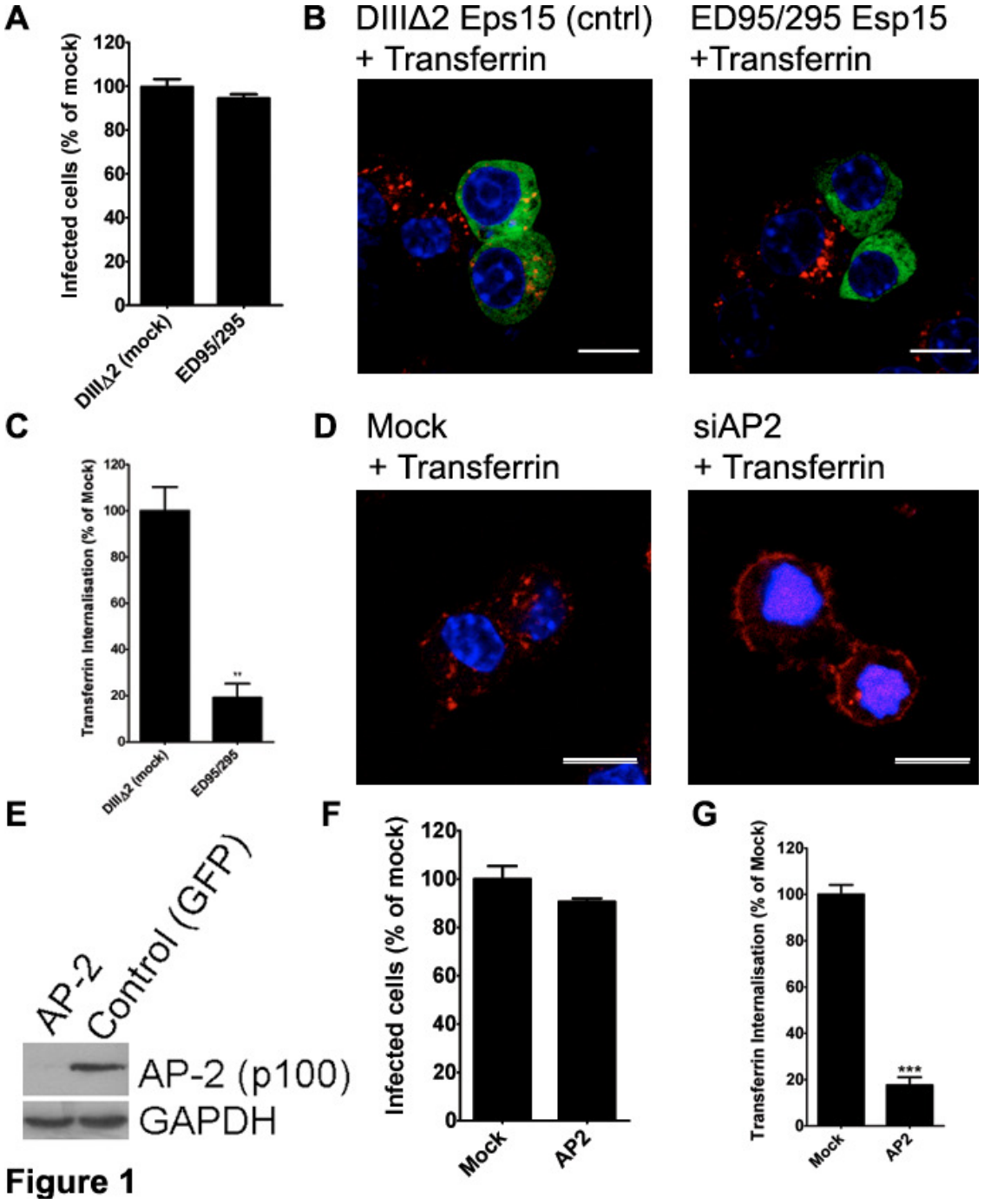
A
Infected cells (% of mock)
120
100
80
60
40
20
0
DIIIΔ2 (mock)
ED95/295
B
DIIIΔ2 Eps15 (cntrl)
+ Transferrin
ED95/295 Esp15
+Transferrin
C
Transferrin Internalisation (% of Mock)
**
DIIIΔ2 (mock)
ED95/295
D
Mock
+ Transferrin
siAP2
+ Transferrin
E
AP-2
Control (GFP)
AP-2 (p100)
GAPDH
F
Infected cells (% of mock)
Mock
AP2
G
Transferrin Internalisation (% of Mock)
***
Mock
AP2

Figure 1

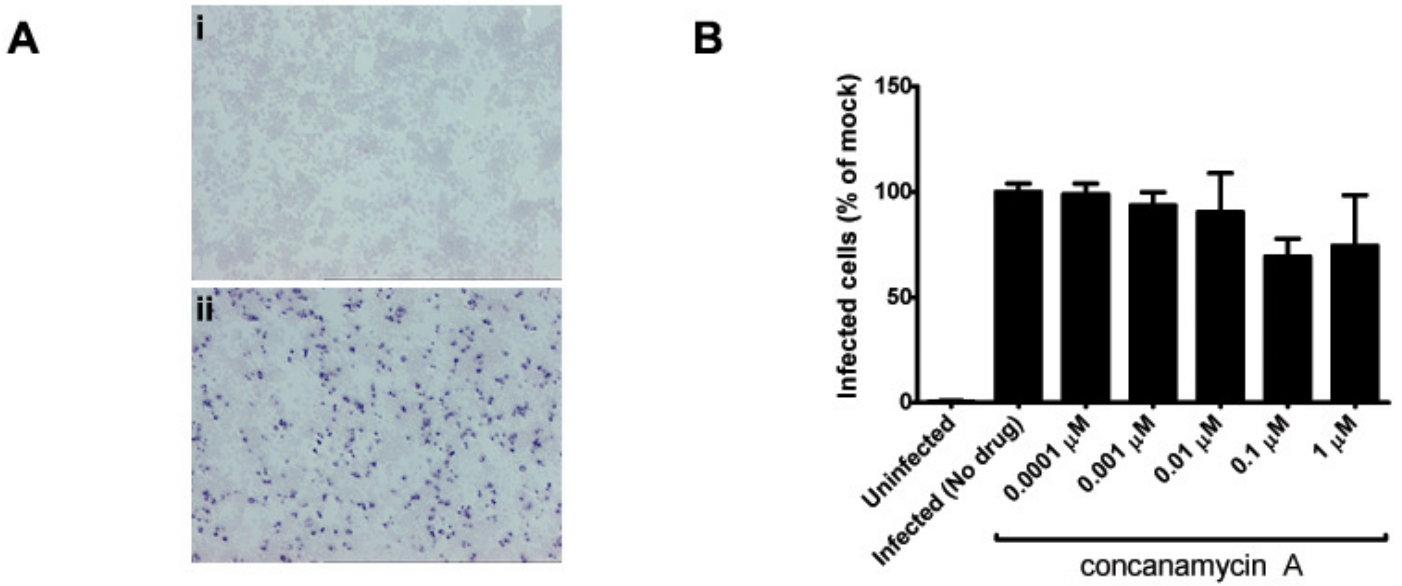
A
i
ii
B
Infected cells (% of mock)
150
100
50
0
Uninfected
Infected (No drug)
0.0001 μM
0.001 μM
0.01 μM
0.1 μM
1 μM
concanamycin A

Figure 2

700

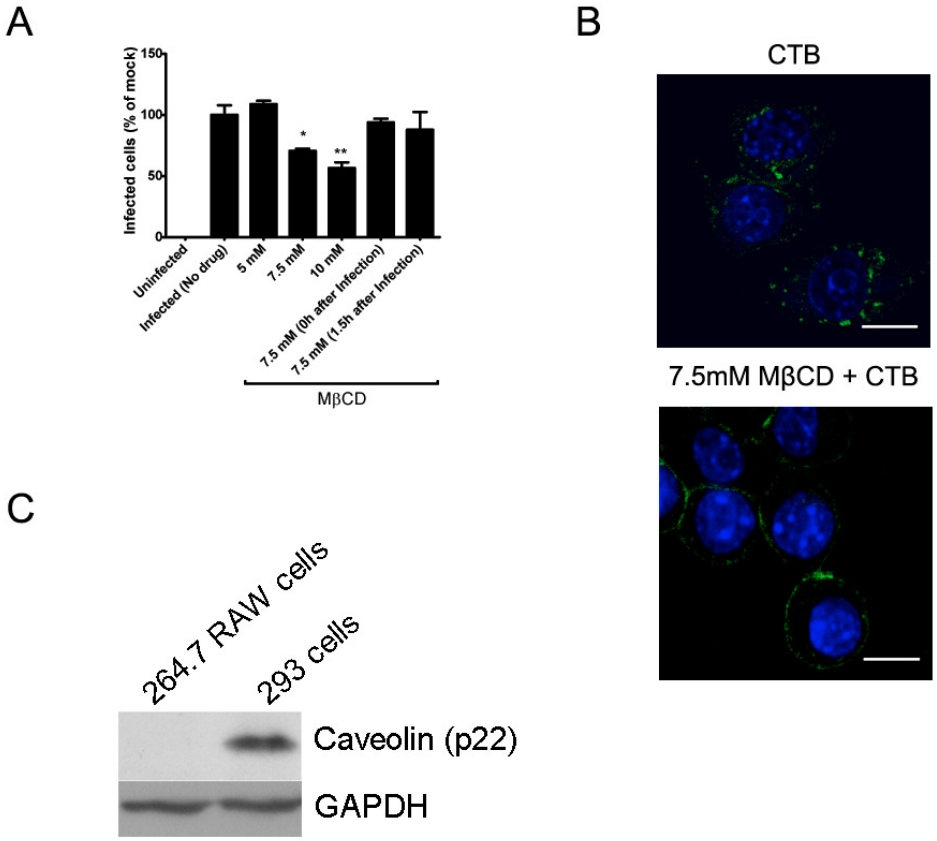
A
Infected cells (% of mock)
150
100
50
0
*
**
Uninfected
Infected (No drug)
5 mM
7.5 mM
10 mM
7.5 mM (0h after Infection)
7.5 mM (1.5h after Infection)
MβCD
B
CTB
7.5mM MβCD + CTB
C
264.7 RAW cells
293 cells
Caveolin (p22)
GAPDH

Figure 3

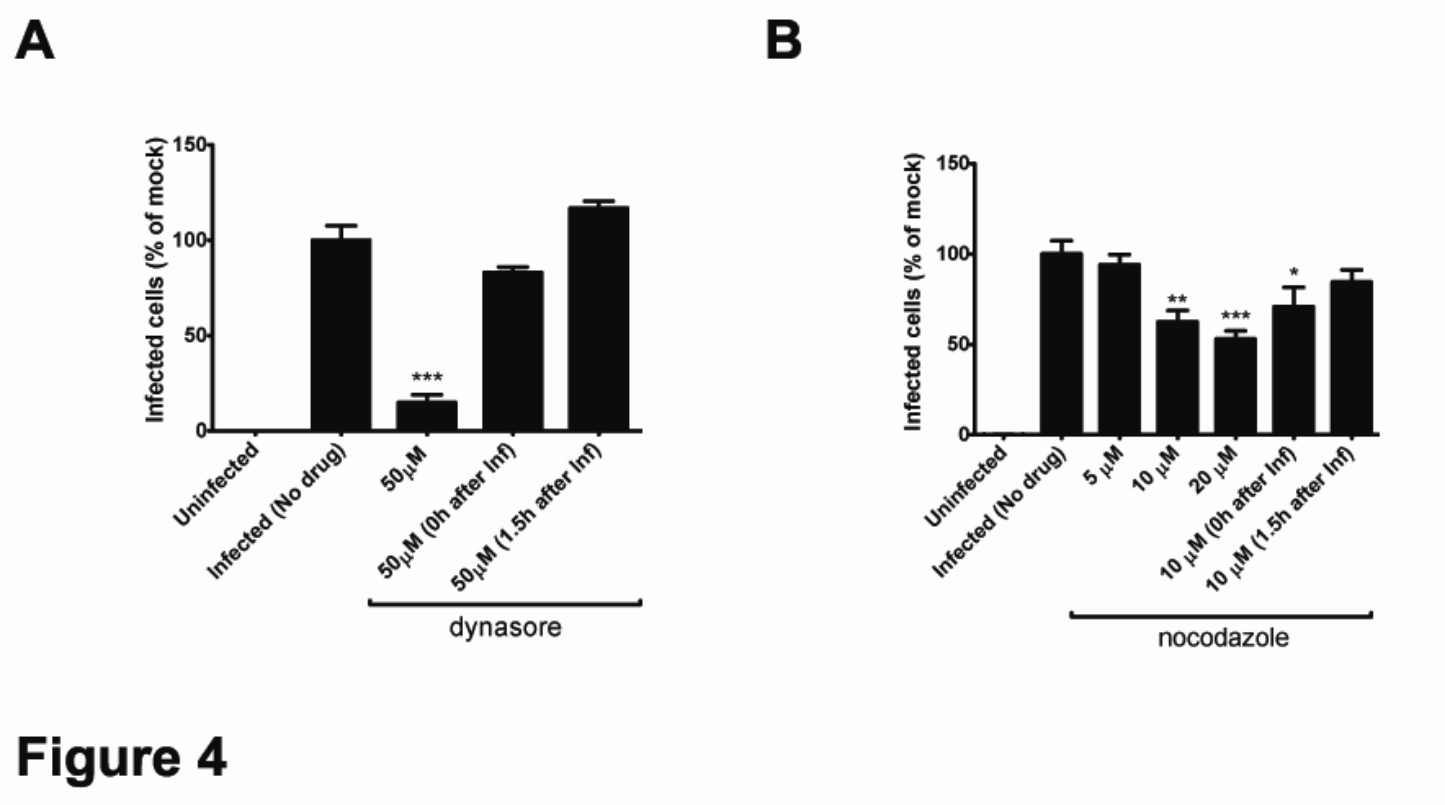
A
Infected cells (% of mock)
150
100
50
0
***
Uninfected
Infected (No drug)
50μM
50μM (0h after Inf)
50μM (1.5h after Inf)
dynasore
B
Infected cells (% of mock)
150
100
50
0
**
***
*
Uninfected
Infected (No drug)
5 μM
10 μM
20 μM
10 μM (0h after Inf)
10 μM (1.5h after Inf)
nocodazole

Figure 4

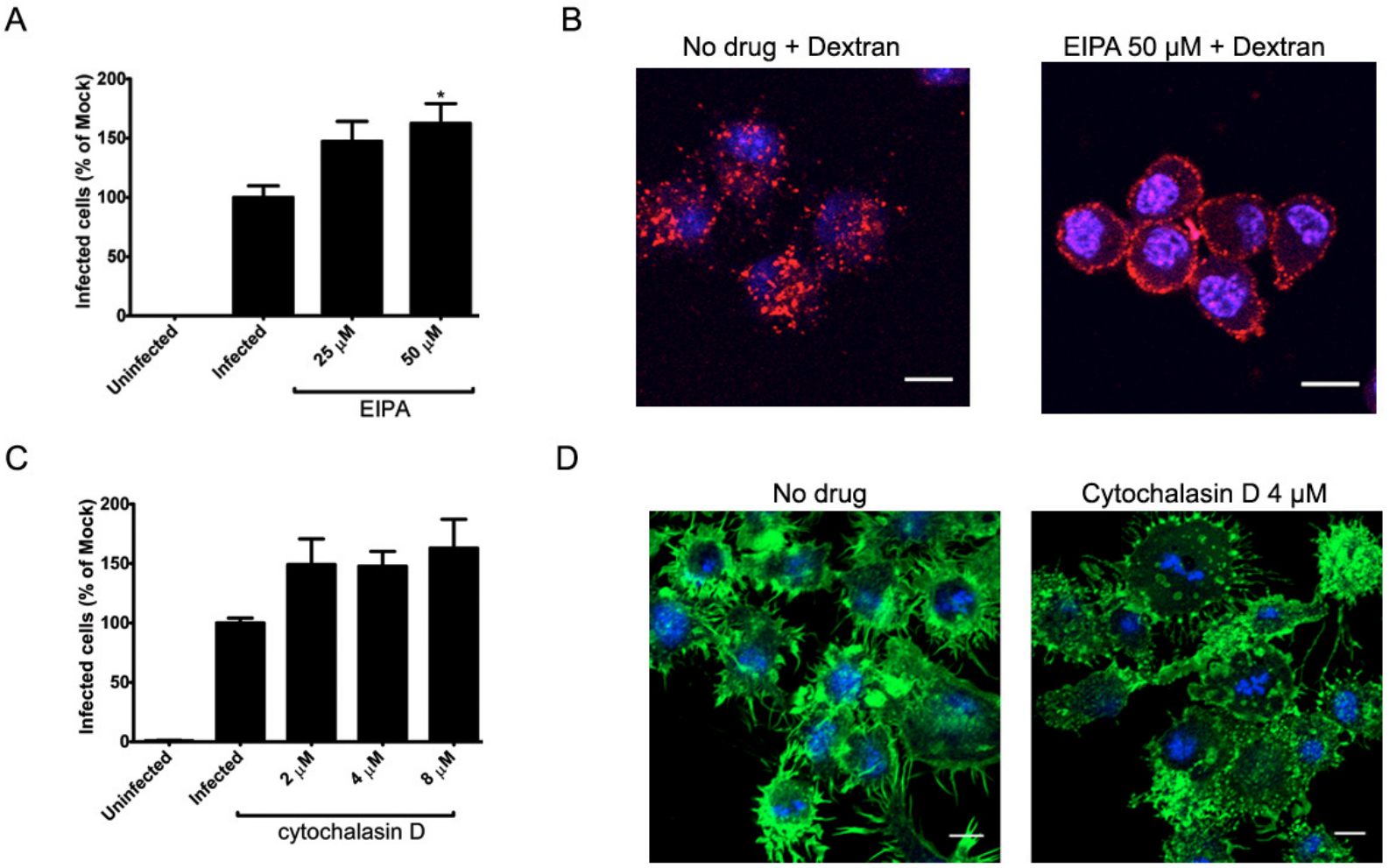
A
Infected cells (% of Mock)
200
150
100
50
0
*
Uninfected
Infected
25 μM
50 μM
EIPA
B
No drug + Dextran
EIPA 50 μM + Dextran
C
Infected cells (% of Mock)
200
150
100
50
0
Uninfected
Infected
2 μM
4 μM
8 μM
cytochalasin D
D
No drug
Cytochalasin D 4 μM

Figure 5

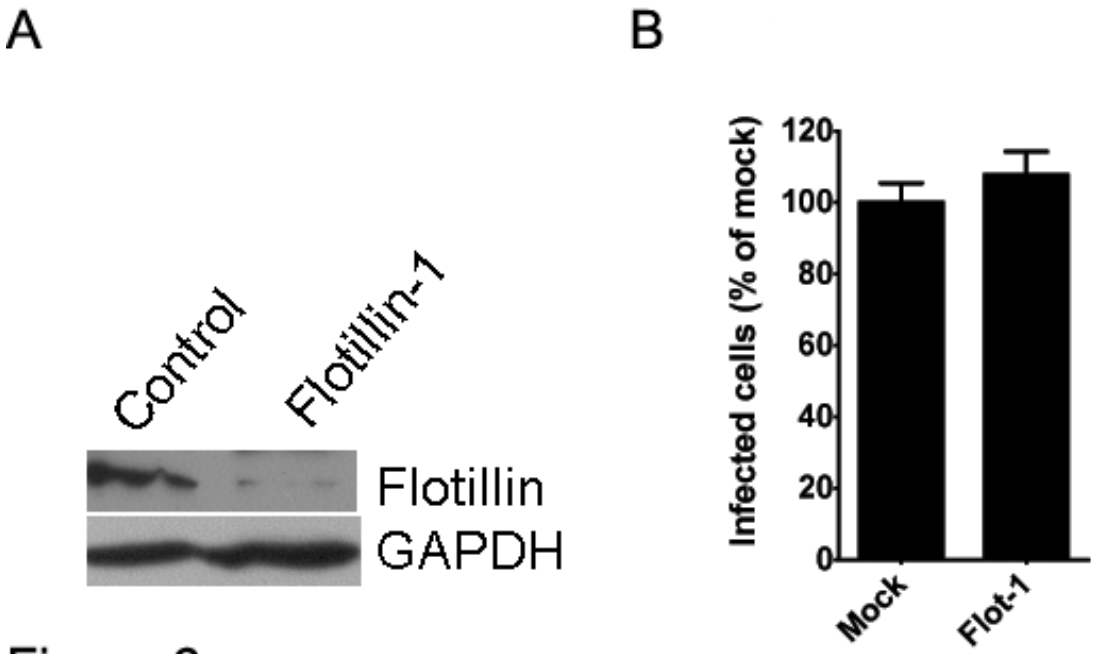
A
Control
Flotillin-1
Flotillin
GAPDH
B
Infected cells (% of mock)
120
100
80
60
40
20
0
Mock
Flot-1

Figure 6

704